Surface and pseudosurface acoustic waves in superlattices

Takashi Aono and Shin-ichiro Tamura
Department of Applied Physics, Hokkaido University, Sapporo 060, Japan
(Received 24 March 1998)

We study theoretically the propagation of surface acoustic waves on the surface of a semi-infinite, periodic superlattice consisting of anisotropic, elastic layers of cubic symmetry. By the use of a transfer-matrix method the dispersion relations of surface modes predominantly polarized in the sagittal plane and also those polarized horizontally, are derived. Pseudosurface-wave (PSW) branches are also found inside the frequency bands of bulk acoustic waves. A remarkable feature is the existence of a PSW branch, which links a surface wave branch below the bulk bands to a branch inside a frequency gap. We present numerical examples for AlAs/GaAs superlattices with an AlAs top surface or a GaAs top surface. Focusing of ballistically propagating surface and pseudosurface waves is also studied. [S0163-1829(98)06832-5]

I. INTRODUCTION

For the last two decades there has been a great deal of work on the vibrational properties in superlattices (SL's). In particular, the propagation characteristics of bulk acoustic phonons in periodic SL's have extensively been studied theoretically and also verified experimentally by phonon spectroscopic and imaging experiments.[1–7] However, there still exists a great deal of activity in this area. A recently studied topic is the problem of phonon surface modes in a semi-infinite SL. A picosecond ultrasonic study has revealed the presence of localized acoustic surface modes in metallic superlattices, which appear in the frequency gaps of the dispersion relation of bulk phonons.[8] The eigenfrequencies of these surface modes coincide well with theoretical calculations based on the transfer-matrix method, though their damping rates are too large to be explained. Also a large time delay is predicted theoretically for the reflection of a phonon from the surface of a SL when its frequency coincides with an eigenfrequency of localized surface vibrational modes.[9]

So far, Djafari-Rouhani and his co-workers have theoretically studied the surface acoustic waves in semi-infinite SL's with a surface parallel or perpendicular to the growth direction.[10–15] However, the majority of the studies employ an isotropic continuum model. The real constituent materials of semiconducting SL's are more or less anisotropic elastically, which gives rise to a considerable change in the acoustic properties. An example is the fact that the direction of the energy flow is not collinear with the wave-vector direction, leading to the focusing and defocusing of ballistically propagating phonons and elastic waves.[16–18] The phonon focusing at solid surfaces has also been predicted and recently verified experimentally.[19–26] In addition, pseudosurface waves that behave like surface waves but have a wave component slowly radiating their energy into the bulk of the solid can exist in an anisotropic surface.[27,28] So far, two previous works on the lattice vibrations at SL surfaces include the effects of anisotropy,[13,14] but the properties of the surface and pseudosurface waves depending on the propagation direction are not fully analyzed.

The purpose of the present work is to investigate theoretically the existence and propagation characteristics of both the surface and pseudosurface acoustic waves on the surface parallel to the layer interfaces of semi-infinite, periodic SL's. We explicitly take account of the elastic anisotropy of the constituent layers and develop in Sec. II the formulation based on the transfer-matrix method. In Sec. III we find the solutions of the surface and pseudosurface waves in SL's and illustrate the band structures, angular dependence of dispersion curves, amplitude profiles, and focusing characteristics. These numerical results are shown for (100) AlAs/GaAs SL's with both AlAs and GaAs surfaces. Conclusions are given in Sec. IV.

II. FORMULATION

We study a semi-infinite SL consisting of alternating layers of A and B materials, which occupies the half space $z>0$ with a flat surface (at $z=0$) parallel to the x-y plane. Figure 1 depicts the SL system under consideration, where A and B layers have thicknesses d_A and d_B, respectively, and the SL period is $D=d_A+d_B$. The displacement vector $\mathbf{U}^A$ and the stress vector $\mathbf{S}^A$ (the component of the stress tensor normal to the surface) in the A layer can be written as

$$\begin{pmatrix} \mathbf{U}_n^A(\mathbf{x},t) \\ \mathbf{S}_n^A(\mathbf{x},t) \end{pmatrix} = \sum_{j=1}^{6} a_n^{(j)} \begin{pmatrix} \mathbf{e}_A^{(j)} \\ \boldsymbol{\sigma}_A^{(j)} \end{pmatrix} \exp(ik_{A,z}^{(j)} z) e^{i(\mathbf{k}_\parallel \cdot \mathbf{x}_\parallel - \omega t)} \equiv \mathbf{W}_n^A(z) e^{i(\mathbf{k}_\parallel \cdot \mathbf{x}_\parallel - \omega t)}, \quad (1)$$

where $\mathbf{x}=(\mathbf{x}_\parallel,z)=(x,y,z)$, n and j are the indices that discriminate the periods (bilayers) and six waves (three pairs of counterpropagating waves) in a layer, respectively, a is an amplitude, $\mathbf{e}$ is a unit polarization vector, $\boldsymbol{\sigma}$ is the stress vector whose components are defined by $\sigma_i=c_{3ilm}k_m e_l$ with c_{ilmn} the stiffness tensor (the summation convention over repeated indices is assumed), $\mathbf{k}=(\mathbf{k}_\parallel,k_z)=(k_x,k_y,k_z)=(k_1,k_2,k_3)$ with $k_z=k_{A,z}^{(j)}$ the wave vector, and ω is the angular frequency. The wave numbers $k_{A,z}^{(j)}(j=1-6)$, which are complex in general, are determined by solving the Christoffel equation

$$(\rho_A \omega^2 \delta_{im} - c_{ilmn}^A k_l k_n) e_m = 0 \quad (i=1,2,3) \quad (2)$$

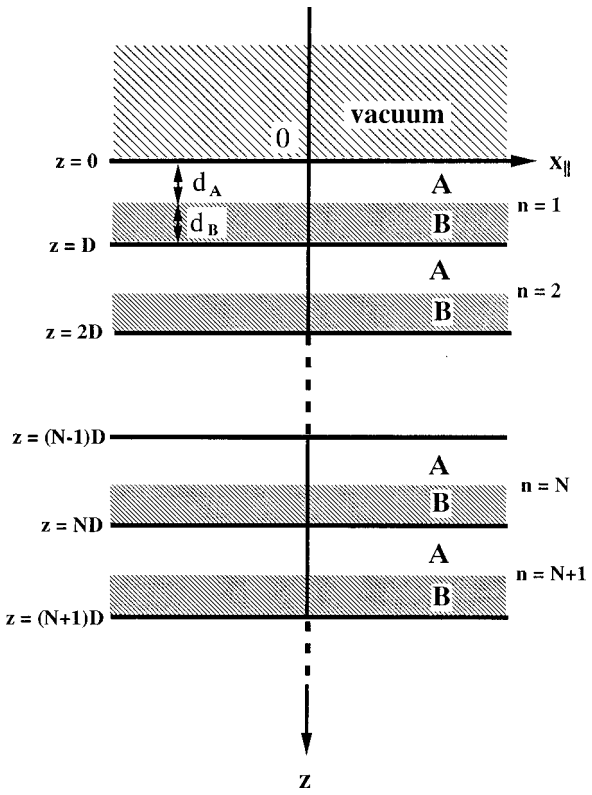

FIG. 1. Schematic of a semi-infinite periodic superlattice consisting of alternating A and B layers with thicknesses d_A and d_B, respectively. The superlattice occupies $z>0$ and has a surface at $z=0$.

for given $\mathbf{k}_\parallel$ (real vector) and ω, where ρ is the mass density. In the B layer the expressions for the displacement and stress vectors are given by Eq. (1) with the amplitude a and index A replaced by b and B, respectively. Hence we write the six-component vector $\mathbf{W}_n^A(z)$ as

$$\mathbf{W}_n^A(z)=\Gamma_A\Phi_A(z)\mathbf{A}_n, \tag{3}$$

where

$$\Gamma_A=\begin{pmatrix} \mathbf{e}_A^{(1)} & \mathbf{e}_A^{(2)} & \cdots & \mathbf{e}_A^{(6)} \\ \boldsymbol{\sigma}_A^{(1)} & \boldsymbol{\sigma}_A^{(2)} & \cdots & \boldsymbol{\sigma}_A^{(6)} \end{pmatrix} \tag{4}$$

and

$$\Phi_A(z)=\begin{pmatrix} \exp(ik_{A,z}^{(1)}z) & 0 & \cdots & 0 \\ 0 & \exp(ik_{A,z}^{(2)}z) & \cdots & 0 \\ \vdots & \vdots & \vdots & \vdots \\ 0 & 0 & \cdots & \exp(ik_{A,z}^{(6)}z) \end{pmatrix} \tag{5}$$

are 6×6 matrices, and

$$\mathbf{A}_n=(a_n^{(1)},a_n^{(2)},\cdots,a_n^{(6)})^t \tag{6}$$

is a six-component column vector.

Now introducing a transfer matrix T that relates $\mathbf{W}_n$ and $\mathbf{W}_{n+1}$ as

$$\mathbf{W}_{n+1}^A(nD)=T\mathbf{W}_n^A[(n-1)D], \tag{7}$$

we find

$$\mathbf{W}_{n+1}^A(nD)=T^n\mathbf{W}_1^A(0). \tag{8}$$

The explicit expression for T is given below. To save the indices we define $\mathbf{W}_{n+1}^A(nD)\equiv\mathbf{w}_n$ and hence $\mathbf{W}_1^A(0)=\mathbf{w}_0$. Thus Eq. (8) is rewritten as

$$\mathbf{w}_n=T^n\mathbf{w}_0. \tag{9}$$

We now look for surface wave solutions satisfying

$$\mathbf{w}_n=\lambda\mathbf{w}_{n-1}, \tag{10}$$

with $|\lambda|<1$. Comparing Eqs. (9) and (10) we find

$$(T-\lambda E)\mathbf{w}_0=0, \tag{11}$$

where E is a 6×6 unit matrix. This eigenvalue equation has six eigenvalues λ_J and the corresponding eigenvectors $\tilde{\mathbf{w}}^{(J)}$ with $J=1$–6. Among those six λ_J we keep three eigenvalues with $|\lambda_J|<1$. Thus, at the surface $z=0$

$$\mathbf{w}_0=\Gamma_A\mathbf{A}_1=\sum_{J=1}^{3}c_J\tilde{\mathbf{w}}^{(J)}, \tag{12}$$

where c_J's are unknown coefficients. If c_J's are known, the amplitude $\mathbf{A}_1$ in the first A layer is determined as

$$\mathbf{A}_1=\sum_{J=1}^{3}c_J\Gamma_A^{-1}\tilde{\mathbf{w}}^{(J)}. \tag{13}$$

Also applying Eq. (8), the amplitude in the $(n+1)$th A layer is given by

$$\mathbf{A}_{n+1}=\sum_{J=1}^{3}c_J(\lambda_J)^n[\Phi_A(nD)]^{-1}\Gamma_A^{-1}\tilde{\mathbf{w}}^{(J)}, \tag{14}$$

The coefficients c_J's are determined from the boundary condition at the surface of the SL. Putting

$$\tilde{\mathbf{w}}^{(J)}=\begin{pmatrix}\mathbf{u}^{(J)}\\ \mathbf{s}^{(J)}\end{pmatrix}, \tag{15}$$

and noting that $\mathbf{w}_0=\mathbf{W}_1^A(0)=[\mathbf{U}_1^A(\mathbf{x}_\parallel,0,t),\mathbf{S}_1^A(\mathbf{x}_\parallel,0,t)]^t$, the boundary condition $\mathbf{S}_1^A(\mathbf{x}_\parallel,0,t)=0$ for the free surface leads to

$$\sum_{J=1}^{3}c_J\mathbf{s}^{(J)}=0. \tag{16}$$

This gives

$$\det\begin{pmatrix} s_1^{(1)} & s_1^{(2)} & s_1^{(3)} \\ s_2^{(1)} & s_2^{(2)} & s_2^{(3)} \\ s_3^{(1)} & s_3^{(2)} & s_3^{(3)} \end{pmatrix}=0. \tag{17}$$

Equation (17) together with the secular equation $\det(T-\lambda E)=0$ determine the frequencies of the surface acoustic mode.

The transfer matrix T is given by the product of the matrices T_A and T_B associated with A and B layers as

$$T=T_BT_A. \tag{18}$$

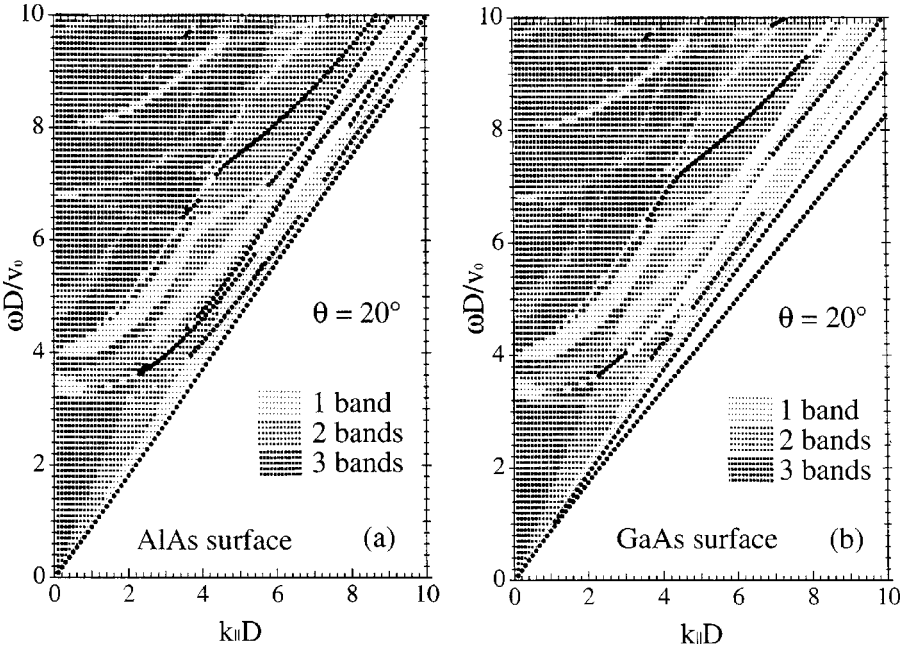

FIG. 2. Band structures and dispersion curves of both the bulk and surface acoustic waves in a periodic superlattice consisting of AlAs and GaAs layers with the same thickness. The propagation direction is rotated 20° from the [100] axis. Filled circles are the surface acoustic waves, and the bulk bands are discriminated by the thickness of dots according to the number of overlapping bands. (a) Surface layer (A layer) is AlAs. (b) Surface layer (A layer) is GaAs. $v_0 = 3.33\times10^5$ cm/s.

The matrices T_A and T_B are constructed as follows:[7] First we introduce 3×3 matrices $e_{\pm}^{(A)}$ and $\sigma_{\pm}^{(A)}$ defined by

$$e_{+}^{(A)} = (\mathbf{e}_A^{(1)}, \mathbf{e}_A^{(2)}, \mathbf{e}_A^{(3)}), \tag{19}$$

$$e_{-}^{(A)} = (\mathbf{e}_A^{(4)}, \mathbf{e}_A^{(5)}, \mathbf{e}_A^{(6)}), \tag{20}$$

$$\sigma_{+}^{(A)} = (\boldsymbol{\sigma}_A^{(1)}, \boldsymbol{\sigma}_A^{(2)}, \boldsymbol{\sigma}_A^{(3)}), \tag{21}$$

$$\sigma_{-}^{(A)} = (\boldsymbol{\sigma}_A^{(4)}, \boldsymbol{\sigma}_A^{(5)}, \boldsymbol{\sigma}_A^{(6)}) \tag{22}$$

and also the diagonal matrices $\phi_{\pm}^{(A)}$ given by

$$\phi_{\pm}^{(A)}(z) = \begin{pmatrix} \exp(\pm ik_{A,z}^{(1)} z) & 0 & 0 \\ 0 & \exp(\pm ik_{A,z}^{(2)} z) & 0 \\ 0 & 0 & \exp(\pm ik_{A,z}^{(3)} z) \end{pmatrix}, \tag{23}$$

where we note $k_{A,z}^{(j+3)} = -k_{A,z}^{(j)}$ for $j = 1$, 2 and 3. With these matrices we next define 6×6 matrices

$$P_A = \begin{pmatrix} e_{+}^{(A)} & e_{-}^{(A)} \\ \sigma_{+}^{(A)} & \sigma_{-}^{(A)} \end{pmatrix}, \tag{24}$$

$$\Phi_A = \begin{pmatrix} \phi_{+}^{(A)}(z) & 0 \\ 0 & \phi_{-}^{(A)}(z) \end{pmatrix}, \tag{25}$$

where $\Phi_A(z)$ is a 6×6 diagonal matrix. Similarly we also define the corresponding matrices P_B and $\Phi_B(d_B)$ with index A replaced by B. Thus, the transfer matrices T_A and T_B are given by

$$T_A = P_A \Phi_A(d_A) P_A^{-1}, \tag{26}$$

$$T_B = P_B \Phi_B(d_B) P_B^{-1}. \tag{27}$$

Note that $\det(T_A) = \det(T_B) = \det(T) = 1$.

III. NUMERICAL RESULTS

We present numerical examples for a periodic SL consisting of alternating AlAs and GaAs layers with the same thicknesses, i.e., $d_A = d_B = D/2$.[29]

A. Surface acoustic waves

In Figs. 2(a) and 2(b) we have plotted the band structures, i.e., the normalized frequency $\omega D/v_0[v_0 = (C_{44}^{\mathrm{GaAs}}/\rho_{\mathrm{GaAs}})^{1/2} = 3.33\times10^5$ cm/s] (Ref. 29) versus normalized wave number $k_{\parallel}D$, of the bulk and surface modes in semi-infinite AlAs/GaAs SL's with an AlAs top surface and a GaAs top surface, respectively. As a typical example, the propagation direction of $\theta = 20°$ rotated from the [100] axis on the surface is chosen. The filled circles are the surface branches that appear either inside the gaps or below the frequency bands of the bulk modes. The existence of surface wave branches inside frequency gaps of the bulk waves is characteristic of the multilayered systems.

Notable results in contrast to the case of surface waves on semi-infinite solids are as follows: (1) Single or double branches are found below the bulk bands depending on whether the surface layer is AlAs or GaAs. (2) High-frequency surface waves are found inside the frequency gaps of the bulk acoustic waves. In order to see the dispersion relations of the surface modes in more detail we have plotted in Figs. 3(a) and 3(b) the angular dependences of the band structures for $k_{\parallel}D = 2$ and $k_{\parallel}D = 10$, respectively.

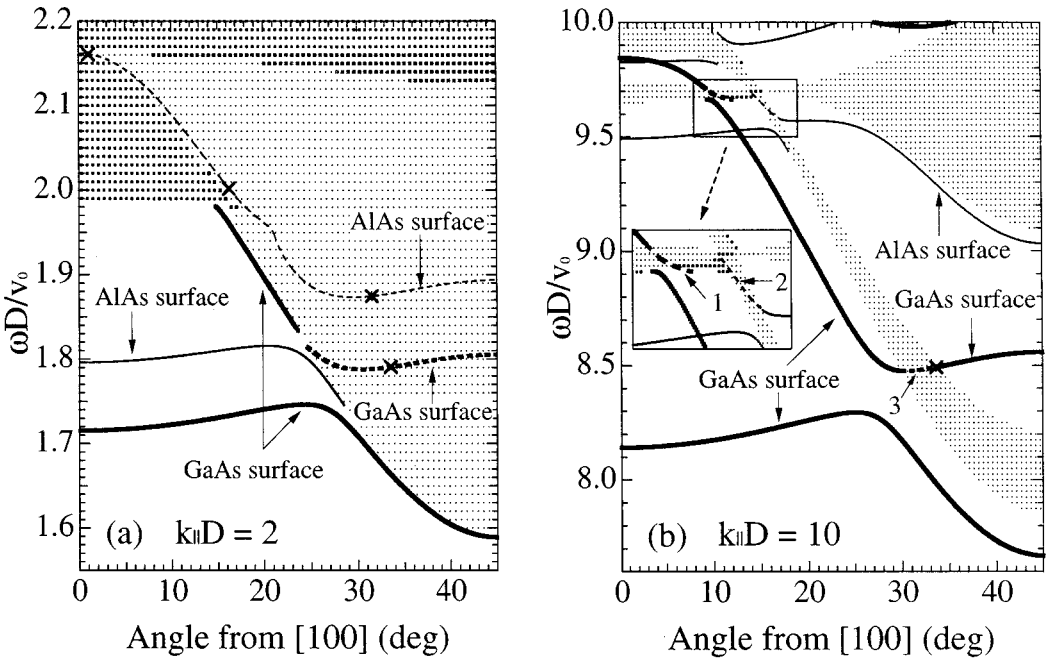

FIG. 3. Angular dependences of the surface and pseudosurface wave frequencies in the periodic superlattice consisting of AlAs and GaAs with the same layer thicknesses. The bold and thin solid (dashed) lines are the surface (pseudosurface) wave branches for the GaAs surface (A=GaAs) and AlAs surface (A=AlAs), respectively. Crosses on the dashed lines are the secluded surface waves on the pseudosurface branches. Dotted regions are the same bulk bands as in Fig. 2. (a) $k_{\parallel}D=2$. (b) $k_{\parallel}D=10$. $v_0=3.33\times10^5$ cm/s.

In Fig. 3(a) for $k_{\parallel}D=2$ we find three surface wave branches below the bulk bands, i.e., two for the GaAs surface and one for the AlAs surface. The lower branch for the GaAs surface corresponds to the Rayleigh wave (RW), which exhibits an angular dependence very similar to the one in semi-infinite GaAs.[19] The upper branch for the GaAs top surface exists only for a restricted range of directions and close to the bulk transverse band with horizontal polarization. Thus, the surface waves on this branch are expected to be also polarized nearly horizontally, that is, they are Love-wave-(LW-) like surface waves.[30] The existence of this upper surface wave branch for the GaAs top surface has been recognized by Nougaoui and Djafari-Rouhani[14] but the details have not been analyzed. The surface wave branch for the AlAs top surface is also RW-like but it disappears at an angle of about $\theta=30°$ by merging with the bulk band. This is consistent with the result of Nougaoui and Djafari-Rouhani[14] found for $k_{\parallel}D=2$.

To confirm the polarizations of the waves in those branches, we have shown in Fig. 4 the profiles of the three components of the displacement vector at $\theta=20°$. We see that the lower two branches are predominantly polarized in the sagittal plane, indicating the RW-like character. However, in the upper branch for the GaAs surface the wave is polarized almost perpendicular to the sagittal plane, i.e., LW-like in character. The slow decay of the displacement amplitude of this mode reflects the fact that this branch is very close to the bulk transverse band. The amplitude decreases more rapidly when the branch is located well below the bulk bands. This can be seen by comparing a similar plot for $k_{\parallel}D=10$ shown in the insets.

No LW-like surface mode exists below the bulk bands for the AlAs surface. This is because the original LW is supported only when the transverse sound velocity of the layer material is slower than that of the semi-infinite substrate.[30] This is also the reason for the fact that the dispersion curve of the RW-like mode below the bulk band is closer to the band edge for the AlAs surface than for the GaAs surface.

More interesting is the band structure for a shorter wavelength shown in Fig. 3(b) for $k_{\parallel}D=10$. In this figure several surface wave branches are found inside the frequency gaps as well as below the frequency band of the bulk waves. In particular, the LW-like upper branch of the surface mode for the GaAs surface is connected to the surface branch inside the frequency gap through the transverse bulk band. Near the [110] direction ($\theta=45°$) the surface waves on this branch are predominantly polarized in the sagittal plane. The branch connecting these surface branches below and inside the bulk bands is a pseudosurface branch which will be discussed in the next subsection.

B. Pseudosurface waves

As in the case for the surface of an anisotropic semi-infinite solid, pseudosurface waves (PSW's) exist on the surface of a SL. The existence of PSW's in SL's was previously recognized by El Boudouti, Djafari-Rouhani, and Nougaoui[15] as resonances in the bulk band of sagittal waves in the isotropic approximation. The PSW's on semi-infinite solids attenuate very slowly with propagation distance because of a weak coupling to a bulk shear mode. The searching procedure for PSW's is essentially the same as that for a semi-infinite solid. That is, we add a small positive imaginary part to $\mathbf{k}_{\parallel}$ by changing $\mathbf{k}_{\parallel}(1+i\varepsilon)$ with $\varepsilon>0$, and find a set of solutions $\lambda_J(J=1-3)$, with $|\lambda_1|,|\lambda_2|<1$ but $|\lambda_3|>1$. These solutions correspond to the wave growing into the SL, and hence should be found inside the frequency bands of a single mode where the propagation of the other two bulk modes are prohibited.

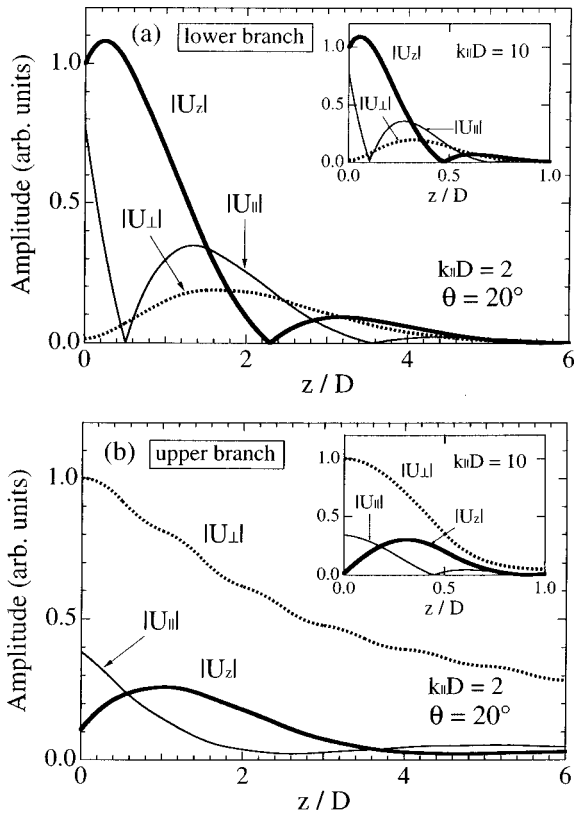

FIG. 4. The amplitudes (absolute values) vs distance (normalized by the unit period D) from the surface for the three components of the lattice displacement: U_z normal to the surface, $U_\parallel$ parallel to the wave vector, and $U_\perp$ perpendicular to the sagittal plane. (a) The lower branch and (b) the upper branch of the surface mode (below bulk bands) for a GaAs surface. The propagation direction is 20° from the [100] axis and $k_\parallel D=2$. The insets show similar plots for $k_\parallel D=10$ with the same direction of propagation.

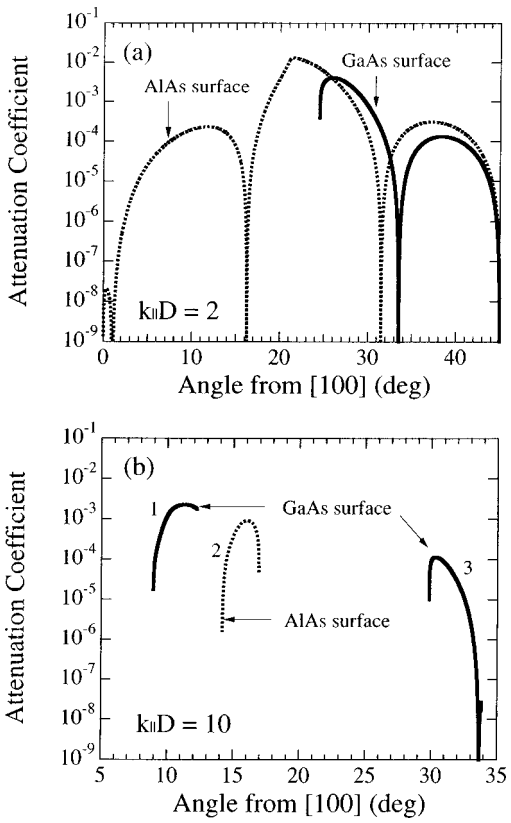

FIG. 5. Attenuation coefficient ε vs propagation direction for the pseudosurface waves shown in Fig. 3. Solid lines are for a GaAs surface and dashed lines are for an AlAs surface. (a) $k_\parallel D=2$. (b) $k_\parallel D=10$. [The numbering 1–3 of the lines corresponds to that for the pseudosurface branches in Fig. 3(a).] Due to the precision of numerical calculations, we could not obtain (for $k_\parallel D=10$, in particular) the solutions for ε in the vicinities of the angles where ε is expected to vanish.

In Fig. 3 the angular dependences of the PSW frequencies are shown by dashed curves. For $k_\parallel D=2$ the PSW branches are found at a relatively low part of the bulk band both for AlAs and for GaAs surfaces. The corresponding attenuation coefficient ε versus propagation direction along the surface has been plotted in Fig. 5 for $k_\parallel D=2$ and $k_\parallel D=10$. This figure shows that ε is quite small, that is, $\sim 10^{-2}$ or less, indicating the small coupling to the bulk wave as expected. Thus the PSW's can propagate along the surface almost unattenuated, and should be observed experimentally just as true surface waves.[31]

From Fig. 3 we also see that at certain isolated directions the waves on the PSW branches become true surface waves ($\varepsilon=0$), for instance, at angles of $\theta\sim 33°$ and $\theta=45°$ from the [100] direction for the GaAs top surface. The waves at these angles (the corresponding positions on the dispersion curves are indicated in Fig. 3 by crosses) are called secluded supersonic surface waves.[32]

An interesting result can be found in Fig. 3(b) for $k_\parallel D=10$. At the lower part of this figure the PSW branch for the GaAs surface links the surface wave branch below the bulk band to that inside a band gap. Also, the upper part of the surface wave branches inside the band gaps continue into the bulk bands as PSW branches both for the AlAs surface and the GaAs surface. Note that only those surface wave

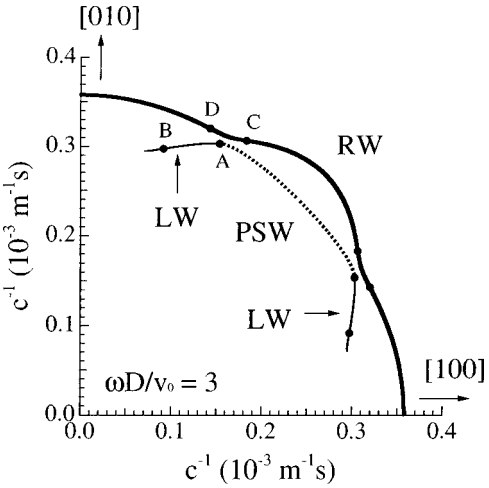

FIG. 6. Slowness curves (the first quadrant) of the Rayleigh-wave-like surface wave (RW, bold solid line), Love-wave-like surface wave (LW, thin solid line), and pseudosurface wave (PSW, dotted line) at $\omega D/v_0=3$. c denotes the phase velocities. The surface layer is GaAs. The points A and B on the LW-like surface branches and C and D on the RW-like surface branches are inflection points which produce cuspidal points on the group-velocity curves.

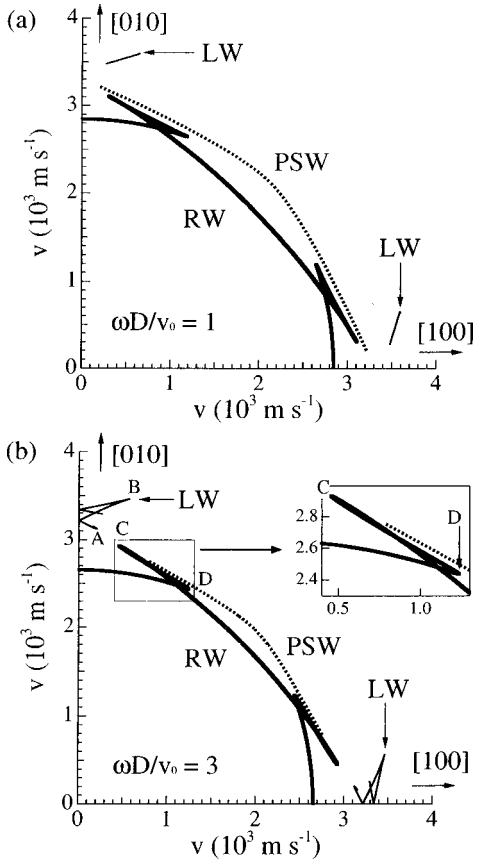

FIG. 7. The group-velocity curves at (a) $\omega D/v_0=1$ and (b) $\omega D/v_0=3$ of the Rayleigh-wave-like surface mode (RW, bold solid line), Love-wave-like surface mode (LW, thin solid line), and pseudosurface mode (PSW, dotted line). The surface layer is GaAs. The cuspidal points $A-D$ of (b) correspond to the inflection points $A-D$ on the slowness curve in Fig. 6.

branches that intersect with a bulk band at a finite angle can continue into the bulk bands as PSW branches. For the surface wave branches that intersect almost tangentially with a bulk band the PSW branches do not continue into this band.

C. Phonon focusing

The acoustic energy associated with elastic wave propagation is carried with the group-velocity. In elastically anisotropic solids the direction of the wave vector and the corresponding group-velocity vector are not collinear in general, leading to the focusing and defocusing of energy flux emanating from a point source. The focusing of the surface acoustic waves is qualitatively understood by looking at the shapes of the constant-frequency (or the slowness) curves $\omega(\mathbf{k}_\parallel)=\omega_0$ (ω_0 is a given frequency) in the wave-vector space whose outward normals give the directions of the group velocities $\mathbf{v}=\nabla_{\mathbf{k}_\parallel}\omega$. The departure of the shape of a slowness curve from a circle gives a measure of the anisotropy of the underlying lattices. In Fig. 6 we have displayed the slowness curves for the RW-like and LW-like surface modes (below the bulk band) as well as for the pseudosurface mode at $\omega D/v_0=3$. The surface layer is assumed to be GaAs. Here, we note that the shapes of these slowness curves do not change markedly even if the frequency is changed.

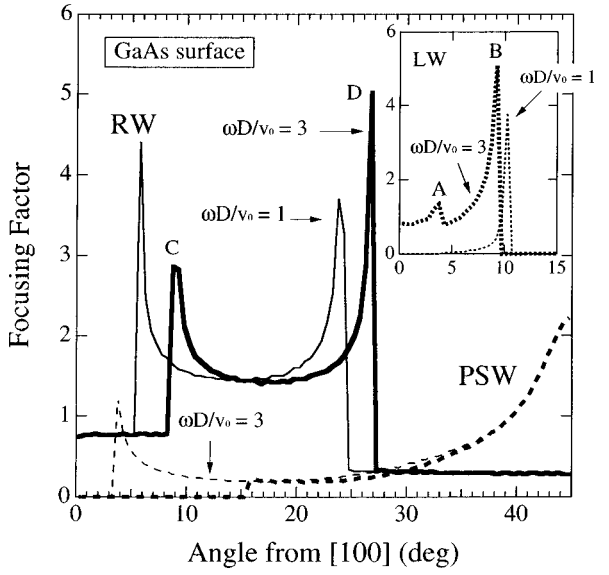

FIG. 8. The focusing factors of the Rayleigh-wave-like surface mode (RW, solid lines), Love-wave-like surface mode (LW, dotted lines in the inset), and pseudosurface mode PSW, (dashed lines) at $\omega D/v_0=1$, and 3. The surface layer is GaAs. The sharp peaks at $A-D$ for $\omega D/v_0=3$ correspond to the cuspidal points $A-D$ of Fig. 7(b) and the inflection points $A-D$ on the slowness curves in Fig. 6. The focusing factors of pseudosurface waves are almost overlapped at angles larger than 16°.

The shapes of the slowness curves of the RW-like mode and pseudosurface mode are qualitatively the same as those on the (100) surfaces of semi-infinite silicon[33] and GaAs.[19] The new feature is the structures due to the LW-like surface mode. The slowness curves of the LW-like mode exist inside the slowness curve of the RW mode and they appear as if they extend from the PSW branch. (This can be also seen in Fig. 3.) A close look at the slowness curves of the LW-like mode reveals that they have both convex and concave regions with inflection points separating these regions. These inflection points (for instance, the points marked A and B, and the points equivalent to them for $\omega D/v_0=3$) produce the cuspidal structures in the group-velocity curves on either side of the [100] direction, as shown in Fig. 7.

The geometrical properties of the slowness and group-velocity curves associated with both the surface and pseudosurface modes should be reflected in the spatial distribution of acoustic energy flux emanating from a point source. We define the focusing factor F, which measures the enhancement of acoustic flux relative to that in an isotropic medium by $F=|\Delta\theta_{\mathbf{k}_\parallel}/\Delta\theta_{\mathbf{v}}|$, where $\Delta\theta_{\mathbf{k}_\parallel}$ is a small angle occupied by the wave vector $\mathbf{k}_\parallel$ in wave-vector space ($\mathbf{k}_\parallel$ space) and $\Delta\theta_{\mathbf{v}}$ is the corresponding small angle subtended by the group-velocity vector $\mathbf{v}$ in real space. In the calculation of F we assume a uniform distribution for the wave-vector directions in $\mathbf{k}_\parallel$ space. Actually, F is given by the sum over $\mathbf{k}_\parallel$ for which the corresponding group-velocity vector $\theta_{\mathbf{v}}$ points the same direction.

Figure 8 shows the angular dependence of the focusing factor F in a given direction $\theta_{\mathbf{v}}$. The surface layer is GaAs. Both the RW-like and LW-like modes have sharp peaks, that is, they have caustics, but PSW's are focused rather weakly in the [110] direction. In contrast to the case of surface

waves on the bulk solids the positions of the caustics change with frequency and an additional caustic (point A) appears for the LW-like mode at higher frequencies.

IV. CONCLUDING REMARKS

We have studied the surface acoustic waves propagating on the surface parallel to the layer interfaces of semi-infinite periodic superlattices, taking account of the elastic anisotropy of the constituent materials. At low frequencies the wavelength of the surface waves is much larger than the layer thickness and the system is essentially equivalent to a semi-infinite anisotropic solid with the same properties as the top layer. Thus, well-known results for surface and pseudo-surface waves in bulk substrates are obtained. However, the situation becomes quite different when the frequency increases and the wavelength becomes comparable to a unit period of the superlattice. We found both RW-like and LW-like surface wave branches inside the gaps of bulk bands as well as below the bulk bands. These surface wave branches exhibit quite different characteristics depending on the material of the surface layer. Below the bulk bands the RW-like surface waves exist both for an AlAs surface and for a GaAs surface, but the LW-like surface wave exists only for the GaAs surface. In the case of a GaAs surface the sound velocity in the surface layer is slower than that in the AlAs layer, and this is consistent with the condition for the existence of Love waves in a system consisting of an elastic layer on a semi-infinite substrate.

We have also searched for PSW branches in AlAs/GaAs SL's. PSW's are found inside bulk bands, and they often appear as if they join up with the surface wave branches below the bulk bands or with those inside the bulk band gaps. A remarkable result is that at large $k_{\|}D$ a PSW branch connects a surface wave branch below the bulk band with a branch inside a band gap. Also the existence of several secluded supersonic surface waves at isolated directions on the PSW branches is confirmed.

Focusing of acoustic energy flux on the surface emanating from a point source is also studied for the branches below the bulk bands and in the low-frequency region. In addition to those of the RW-like mode, sharp focusings with caustics are found for the LW-like mode near the [110] axis. The theoretical results presented in this study could be verified by observing focusing effects with optical excitation of incoherent surface acoustic waves in the 50-MHz range[21] or through the excitation of coherent surface acoustic waves in the 10-MHz range with focused immersion transducers.[23]

ACKNOWLEDGMENTS

The authors would like to thank O. B. Wright for a critical reading of the manuscript. This work was supported in part by the Grant-in-Aid for Scientific Research from the Ministry of Education, Science and Culture of Japan (Grant No. 09640385).

[1] A.S. Barker, Jr., J.L. Merz, and A.C. Gossard, Phys. Rev. B **17**, 3181 (1978).
[2] V. Narayanamurti, H.L. Störmer, M.A. Chin, A.C. Gossard, and W. Wiegmann, Phys. Rev. Lett. **43**, 2012 (1979).
[3] S. Tamura and J.P. Wolfe, Phys. Rev. B **35**, 2528 (1987).
[4] D.C. Hurley, S. Tamura, J.P. Wolfe, and H. Morkoç, Phys. Rev. Lett. **58**, 2446 (1987).
[5] O. Koblinger, J. Mebert, E. Dittrich, S. Döttinger, W. Eisenmenger, P.V. Santos, and L. Ley, Phys. Rev. B **35**, 9372 (1987).
[6] P.V. Santos, L. Ley, J. Mebert, and O. Koblinger, Phys. Rev. B **36**, 1306 (1987).
[7] S. Tamura, D.C. Hurley, and J.P. Wolfe, Phys. Rev. B **38**, 1427 (1988).
[8] W. Chen, Y. Lu, H.J. Maris, and G. Xiao, Phys. Rev. B **50**, 14 506 (1994).
[9] S. Mizuno and S.I. Tamura, Phys. Rev. B **53**, 4549 (1996).
[10] R.E. Camley, B. Djafari-Rouhani, L. Dobrzynski, and A.A. Maradudin, Phys. Rev. B **27**, 7318 (1983).
[11] B. Djafari-Rouhani, L. Dobrzynski, O. Hardouin Duparc, R.E. Camley, and A.A. Maradudin, Phys. Rev. B **28**, 1711 (1983).
[12] B. Djafari-Rouhani, A.A. Maradudin, and R.F. Wallis, Phys. Rev. B **29**, 6454 (1984).
[13] A. Nougaoui and B. Djafari-Rouhani, Surf. Sci. **199**, 623 (1988).
[14] A. Nougaoui and B. Djafari-Rouhani, J. Electron Spectrosc. Relat. Phenom. **45**, 197 (1987).
[15] E.H. El Boudouti, B. Djafari-Rouhani, and A. Nougaoui, Phys. Rev. B **51**, 13 801 (1995).
[16] B. Taylor and H.J. Maris, Phys. Rev. Lett. **23**, 416 (1969); Phys. Rev. B **3**, 1462 (1961).
[17] H.J. Maris, J. Acoust. Soc. Am. **50**, 812 (1971).
[18] G. A. Northrop and J. P. Wolfe, in *Nonequilibrium Phonon Dynamics*, edited by W. E. Bron (Plenum, New York, 1985), Chap. 5.
[19] S. Tamura and K. Honjo, Jpn. J. Appl. Phys., Suppl. 3, **20**, 17 (1980).
[20] R.E. Camley and A.A. Maradudin, Phys. Rev. B **27**, 1959 (1983).
[21] Al. A. Kolomenskii and A.A. Maznev, Pis'ma Zh. Éksp. Teor. Fiz. **53**, 403 (1991) [JETP Lett. **53**, 423 (1991)]; Phys. Rev. B **48**, 14 502 (1993).
[22] A.A. Maznev, Al. A. Kolomenskii, and P. Hess, Phys. Rev. Lett. **75**, 3332 (1995).
[23] R.E. Vines, S.I. Tamura, and J.P. Wolfe, Phys. Rev. Lett. **74**, 2729 (1995); **75**, 1873(E) (1995).
[24] S. Tamura, R.E. Vines, and J.P. Wolfe, Phys. Rev. B **54**, 5151 (1996).
[25] C. Höss and H. Kinder, Physica B **219-220**, 706 (1996).
[26] T. Aono and S. Tamura, Phys. Rev. B **55**, 6754 (1997).
[27] T.C. Lim and G.W. Farnell, J. Acoust. Soc. Am. **45**, 845 (1969).
[28] G. W. Farnell , in *Physical Acoustics VI*, edited by W. P. Mason and R. N. Thurston (Academic, New York, 1970), p. 109.
[29] We use the elastic constants $C_{11}=12.02, C_{12}=5.70$, and $C_{44}=5.89$ (in units of 10^{11} dyn/cm^2) and mass density $\rho=3.76$ g/cm^3 for AlAs, and $C_{11}=11.88$, $C_{12}=5.38$, and $C_{44}=5.94$ (in units of 10^{11} dyn/cm^2) and mass density $\rho=5.36$ g/cm^3 for GaAs. The transverse sound velocities along the [100] directions are 3.96×10^5 cm/s in AlAs and 3.33×10^5 cm/s in GaAs.

[30] Love wave is the surface wave that exists in the system with an elastic layer on a semi-infinite substrate. See, for example, G. W. Farnell and E. L. Adler, in *Physical Acoustics XI*, edited by W. P. Mason and R. N. Thurston (Academic, New York, 1972), p. 35.

[31] F.R. Rollins, Jr., T.C. Lim, and G.W. Farnell, Appl. Phys. Lett. **12**, 236 (1968).

[32] A.A. Mazunev and A.G. Every, Phys. Lett. A **197**, 423 (1995).

[33] S. Tamura and M. Yagi, Phys. Rev. B **49**, 17 378 (1994).